

Different routes to charge disproportionation in perovskites-type Fe oxides

J. Matsuno,* T. Mizokawa, and A. Fujimori

*Department of Physics and Department of Complexity Science and Engineering,
University of Tokyo, Bunkyo-ku, Tokyo 113-0033, Japan*

Y. Takeda

Department of Chemistry, Mie University, Tsu 514-8507, Japan

S. Kawasaki and M. Takano

Institute of Chemical Research, Kyoto University, Uji, Kyoto 611-0011, Japan

(Dated: February 1, 2008)

Iron perovskites CaFeO_3 and $\text{La}_{0.33}\text{Sr}_{0.67}\text{FeO}_3$ show charge disproportionation, resulting in charge-ordered states with $\text{Fe}^{3+}:\text{Fe}^{5+} = 1:1$ and $= 2:1$, respectively. We have made photoemission and unrestricted Hartree-Fock band-structure calculation of CaFeO_3 and compared it with $\text{La}_{0.33}\text{Sr}_{0.67}\text{FeO}_3$. With decreasing temperature, a gradual decrease of the spectral weight near the Fermi level occurred in CaFeO_3 as in $\text{La}_{0.33}\text{Sr}_{0.67}\text{FeO}_3$ although lattice distortion occurs only in CaFeO_3 . Hartree-Fock calculations have indicated that both the breathing and tilting distortions are necessary to induce the charge disproportionation in CaFeO_3 , while no lattice distortion is necessary for the charge disproportionation in $\text{La}_{0.33}\text{Sr}_{0.67}\text{FeO}_3$.

PACS numbers: 71.27.+a, 75.25.+z, 71.15.-m, 79.60.Bm

Recently charge ordering phenomena in transition-metal oxides have been extensively studied, particularly in relation to charge stripes in the high- T_C cuprates [1] and giant magnetoresistance in the manganites [2]. Charge ordering in highly covalent transition-metal oxides containing d^4 (Fe^{4+} , Mn^{3+}) or d^7 (Ni^{3+}) ions often exhibit so-called charge disproportionation, in which a charge state is thought to be separated into two different charge states as $2d^n \rightarrow d^{n-1} + d^{n+1}$. A clear fingerprint of charge disproportionation is the breathing-type distortion of metal-oxygen octahedra since the different charge states of the transition-metal ion take different ionic radii. Indeed, a breathing-type lattice distortion has been found for $\text{YNi}^{3+}\text{O}_3$ [3], $\text{NdNi}^{3+}\text{O}_3$ [4] and $\text{CaFe}^{4+}\text{O}_3$ by neutron diffraction studies [5, 6] and a thermally fluctuating charge disproportionated state has been postulated for LaMnO_3 at high temperatures [7]. However, charge disproportionation in $\text{La}_{1-x}\text{Sr}_x\text{FeO}_3$ with $x \simeq 0.7$, which occurs as a first-order phase transition from the paramagnetic average-valence state ($\text{Fe}^{\sim 3.7+}$) above 200 K to the antiferromagnetic charge-disproportionated state ($\text{Fe}^{3+}:\text{Fe}^{5+} = 2:1$) below that temperature [8], is not accompanied by an appreciable lattice distortion [9] although an electron diffraction study has shown extra spots [10] and two charge states of Fe with different hyperfine fields have been detected by Mössbauer spectroscopy [8]. The neutron diffraction study of $\text{La}_{0.3}\text{Sr}_{0.7}\text{FeO}_3$ [9] has revealed a spin-density wave (SDW) of six-fold periodicity along the $\langle 111 \rangle$ direction with two inequivalent spin states of Fe, suggesting a charge-density wave (CDW) of three-fold periodicity along the same direction.

Recent photoemission studies have revealed that the

electronic structure of Fe^{4+} oxides is rather unique: the charge-transfer energy Δ , the energy required to transfer an electron from the oxygen p to the Fe $3d$ level, is extremely negative (~ -3 eV including Hund's coupling energy) [11], and the ground state of the formal Fe^{4+} (" d^4 ") state is in fact dominated by the $d^5\bar{L}$ configuration, where \bar{L} denotes a hole in the oxygen $2p$ band. The charge disproportionation is therefore more correctly described as $2d^5\bar{L} \rightarrow d^5\bar{L}^2 + d^5$ rather than $2d^4 \rightarrow d^3 + d^5$. To understand the interesting physical properties of Fe^{4+} oxides such as the helical antiferromagnetic metallic state in SrFeO_3 [12], the Co-substitution induced ferromagnetism in $\text{SrFe}_{1-x}\text{Co}_x\text{O}_3$ [13, 14], and magnetic and electric phase transitions under high pressure [15, 16, 17], therefore, one has to take into account the negative Δ , namely, the oxygen-hole character of charge carriers. Especially, the $d^5\bar{L}$ ground state naturally explains the fact that SrFeO_3 shows no charge disproportionation yet no Jahn-Teller effect since the d^4 ion necessarily undergoes a Jahn-Teller distortion.

In a recent photoemission and unrestricted Hartree-Fock band-structure calculation study of $\text{La}_{1-x}\text{Sr}_x\text{FeO}_3$ [18], we have shown that the charge disproportionation is purely electronically driven and that the ordering of oxygen holes plays an important role in the charge disproportionated state of $\text{La}_{0.33}\text{Sr}_{0.67}\text{FeO}_3$. In this Letter, we present a photoemission study of CaFeO_3 , which unlike $\text{La}_{0.33}\text{Sr}_{0.67}\text{FeO}_3$ shows a breathing-type lattice distortion in the charge disproportionated state. Using photoemission we have studied how the charge disproportionation influences the electronic structure near the Fermi level (E_F) in comparison with $\text{La}_{0.33}\text{Sr}_{0.67}\text{FeO}_3$. We have also

performed unrestricted Hartree-Fock band-structure calculations on CaFeO_3 taking into account the realistic lattice distortion. Based on those results, different driving mechanisms are proposed for the charge disproportionation in the seemingly very similar systems CaFeO_3 and $\text{La}_{0.33}\text{Sr}_{0.67}\text{FeO}_3$.

A polycrystalline sample of CaFeO_3 was prepared by a solid state reaction and a subsequent treatment under high-pressure oxygen [13]. The electrical resistivity of the present CaFeO_3 sample is shown in Fig. 1 and is compared with that of $\text{La}_{1-x}\text{Sr}_x\text{FeO}_3$ ($x = 0.67$) [18]. It shows a gradual increase below the anomaly at 290 K due the gradual charge disproportionation $2\text{Fe}^{4+} \rightarrow \text{Fe}^{5+} + \text{Fe}^{3+}$ while no anomaly due to the antiferromagnetic ordering is seen at the Néel temperature $T_N = 115$ K.

Ultraviolet photoemission (UPS) measurements were made using the He I resonance line ($h\nu = 21.2$ eV). The He I spectra have been corrected for the He I* satellite. In order to calibrate binding energies and to estimate the instrumental resolution, gold was evaporated on the sample surface after each series of measurements. The energy resolution was 48 meV. The samples were repeatedly scraped *in situ* with a diamond file. We have adopted the spectra taken within 40 minutes after scraping and the reproducibility of the spectra was confirmed by repeated measurements.

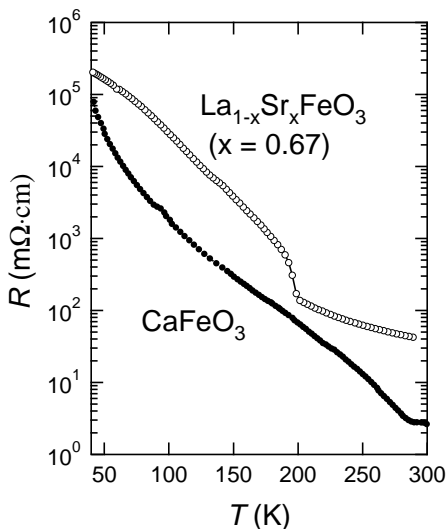


FIG. 1: Electrical resistivities of CaFeO_3 and $\text{La}_{0.33}\text{Sr}_{0.67}\text{FeO}_3$.

Figure 2 shows the temperature dependence of the He I spectra of CaFeO_3 near E_F . The spectra have been normalized to the integrated intensity of the entire valence band. A clear change in the intensity from the Fermi level to 0.4 eV below it has been observed as in the case of $\text{La}_{0.33}\text{Sr}_{0.67}\text{FeO}_3$. One can see that the spectral weight near E_F show a gradual decrease of

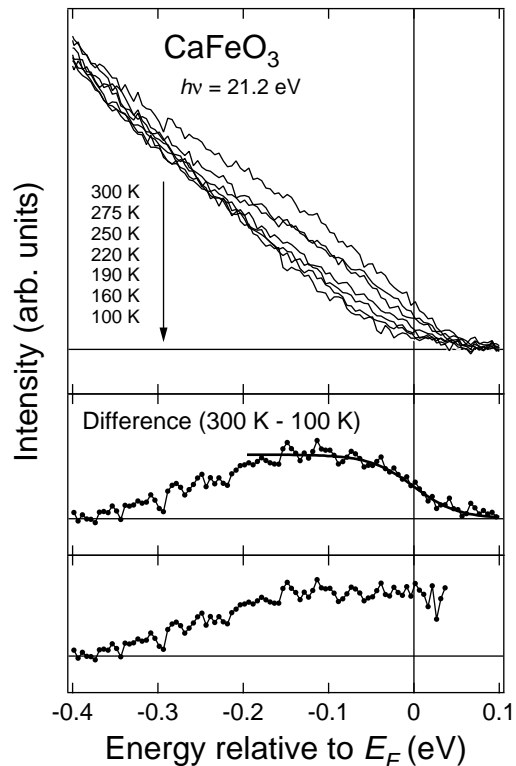


FIG. 2: Photoemission spectra of CaFeO_3 . Top: Spectra taken at various temperatures. Middle: Difference spectrum between 300 K and 100 K. The solid curve is the Fermi-Dirac distribution function at 300 K convoluted with the instrumental resolution. Bottom: The same difference spectrum divided by the Fermi-Dirac distribution function.

the spectral weight with decreasing temperature. The most prominent temperature dependence occurs just below 300 K, followed by more gradual changes below ~ 270 K. In order to illustrate this, we have plotted the spectral weight integrated from -0.20 to $+0.05$ eV as a function of temperature in Fig. 3(a), where the previous result on $\text{La}_{0.33}\text{Sr}_{0.67}\text{FeO}_3$ is also plotted [18]. One can see a more gradual decrease as a function of temperature in CaFeO_3 than in $\text{La}_{0.33}\text{Sr}_{0.67}\text{FeO}_3$ corresponding to the more gradual change in the electrical resistivity below the charge disproportionation temperature, although the total spectral change in the wide temperature range is similar between the two systems. We also note that this temperature dependence of the spectral weight is qualitatively similar to the temperature dependence of the Fe-O bond length [6] as shown in Fig. 3(b), suggesting that the lattice deformation is related to the change of the photoemission spectra in CaFeO_3 . It is remarkable that, although $\text{La}_{0.33}\text{Sr}_{0.67}\text{FeO}_3$ shows negligibly small structural changes across the transition [9], it shows spectral changes as strong as CaFeO_3 . These observations imply different mechanisms for the charge disproportionation

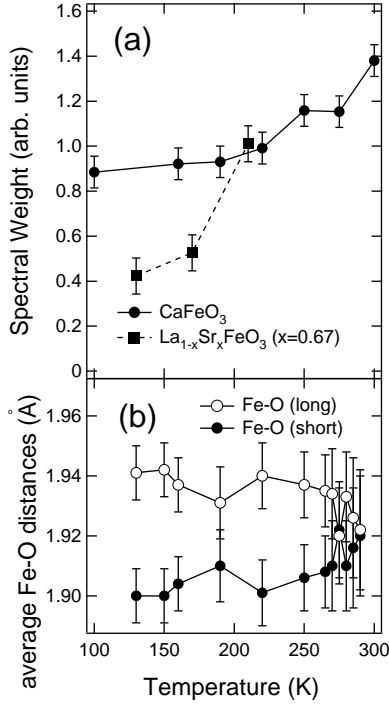


FIG. 3: (a) Spectral weight integrated from -0.20 to $+0.05$ eV for CaFeO_3 and $\text{La}_{0.33}\text{Sr}_{0.67}\text{FeO}_3$ [18] as functions of temperature. (b) Average Fe-O bond lengths observed by neutron diffraction [6].

between the two systems.

In Fig. 2, the difference spectrum between 300 K and 100 K is compared with the Fermi-Dirac distribution function $f_D(\epsilon)$ at $T = 300$ K. The difference spectrum seems to agree rather well with $f_D(\epsilon)$ near E_F . This is different from $\text{La}_{0.33}\text{Sr}_{0.67}\text{FeO}_3$, which shows a pseudo-gap-like behavior at E_F . In order to clarify this, the difference spectrum divided by the Fermi-Dirac distribution function is also shown in the bottom panel. The obtained spectral DOS is nearly flat around the E_F , in contrast to the corresponding spectrum for $\text{La}_{0.33}\text{Sr}_{0.67}\text{FeO}_3$, where a pseudo-gap-like DOS has been observed [18]. This is consistent with the transport properties, which show more conducting and metallic behavior in CaFeO_3 than in $\text{La}_{0.33}\text{Sr}_{0.67}\text{FeO}_3$ above the transition temperature.

In order to study the driving force for the phase transition and the origin of the band gap below the transition temperature in CaFeO_3 , we have carried out unrestricted Hartree-Fock calculations for the multi-band d - p lattice model, in which the full degeneracy of the Fe $3d$ and oxygen $2p$ orbitals are taken into account [19]. Parameters in the model are the charge-transfer energy Δ , the multiplet averaged d - d Coulomb interaction U and Slater-Koster parameters ($pd\sigma$), ($pd\pi$), ($pp\sigma$) and ($pp\pi$), which represent transfer integrals between the transition metal $3d$ and oxygen $2p$ orbitals. The values of Δ , U and ($pd\sigma$)

were chosen to be 0, 6 and -1.8 eV, respectively. The ratio ($pd\sigma$)/($pd\pi$) was fixed at -2.16 and ($pp\sigma$) and ($pp\pi$) at -0.60 and 0.15 eV, respectively [20].

First, in analogy with $\text{LaSr}_2\text{Fe}_3\text{O}_9$ (a supercell model for $\text{La}_{0.33}\text{Sr}_{0.67}\text{FeO}_3$) [18], where charge ordering with $\text{Fe}^{3+} : \text{Fe}^{5+} = 2 : 1$ causes an SDW with six-fold periodicity along the $\langle 111 \rangle$ direction [Fig. 4(a)], we assumed an SDW with four-fold periodicity, namely $\uparrow\uparrow\downarrow\downarrow$, for CaFeO_3 , where ordering with $\text{Fe}^{3+} : \text{Fe}^{5+} = 1 : 1$ occurs in the same direction. This assumption is compatible with the alternating charge order of Fe^{3+} and Fe^{5+} in CaFeO_3 . Under this assumption we obtained an insulating solution but this was not a disproportionated one. The reason why we could not explain both charge-ordered and insulating ground state within the $\uparrow\uparrow\downarrow\downarrow$ model is schematically shown in Fig. 4(b). The tendency that holes enter oxygen orbitals between the iron sites of the parallel spins also holds in this case, but all the iron sites become equivalent in spite of the hole ordering in this geometry, as can be seen from Fig. 4(b). Thus the origin of the disproportionation in CaFeO_3 and in $\text{LaSr}_2\text{Fe}_3\text{O}_9$ cannot be the same. In other words, the kinetic exchange interaction derived from the particular magnetic structure as in the case of $\text{La}_{0.33}\text{Sr}_{0.67}\text{FeO}_3$ cannot drive the charge disproportionation in CaFeO_3 .

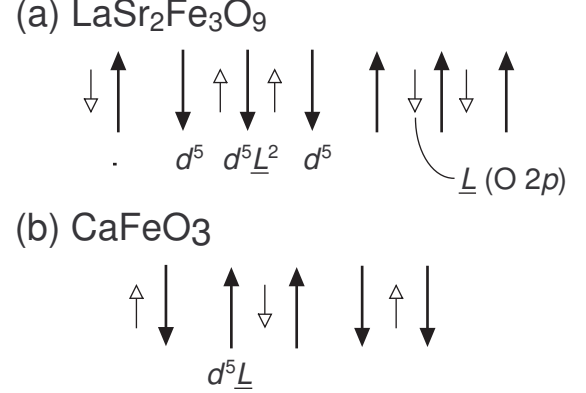


FIG. 4: Schematic descriptions of the spin and charge configurations in $\text{LaSr}_2\text{Fe}_3\text{O}_9$ ($\text{La}_{0.33}\text{Sr}_{0.67}\text{FeO}_3$) (a) and CaFeO_3 (b). Black and white arrows represent the spins at the Fe sites and those of the oxygen holes, respectively.

Then we introduced the lattice distortion in CaFeO_3 explicitly because in CaFeO_3 , lattice distortion has been found to be substantial unlike $\text{La}_{0.33}\text{Sr}_{0.67}\text{FeO}_3$. CaFeO_3 has the GdFeO_3 -type tilting distortion as well as the breathing distortion [5, 6, 21] and the Fe-O-Fe bond angle is determined to be $\sim 158^\circ$. In order to take into account these distortions, a unit cell has been selected as containing four FeO_6 octahedra. The breathing distortion, which results in two kinds of Fe-O bond lengths, has been treated by scaling the transfer integrals with respect

\angle Fe-O-Fe	$R = 1$	$R = 1.022$	$R = 1.043$
180°	0	0	190
158°	0	30	300

TABLE I: Band gap in units of meV for various breathing (represented by $R = d_{\text{long}}/d_{\text{short}}$) and tilting (represented by Fe-O-Fe) distortions for CaFeO_3 . $R = 1.022$ and Fe-O-Fe = 158° are the experimental values.

to the bond lengths (d) following Harrison's rule [22] ($pd\sigma \propto d^{-3.5}$). In order to simulate the effect of both the breathing and the tilting, we calculated the magnitude of the band gap as a function of the degree of the breathing distortion $R = d_{\text{long}}/d_{\text{short}}$ and the Fe-O-Fe bond angle. As for the magnetic structure, we assumed the ferromagnetic structures considering that the spin alignment between neighboring iron sites is almost ferromagnetic in the screw antiferromagnetic structure with a long wave vector [= $0.161(111)2\pi/a$] observed in CaFeO_3 [5]. The results are shown in Table I. We have obtained the charge-disproportionated solution for $R \neq 1$ as expected. The experimental values for CaFeO_3 are $R = 1.022$ and $\angle\text{Fe-O-Fe} = 158^\circ$ for CaFeO_3 , however, the breathing distortion of $R = 1.022$ alone or the tilting of $\angle\text{Fe-O-Fe} = 158^\circ$ alone does not open a gap although Hartree-Fock calculations tend to overestimate band gaps. In order to open a band gap (and to lower the total energy of the system), the two types of lattice distortions should occur simultaneously. If the bond angle is 180° as in the case of SrFeO_3 , one needs an unreasonably large breathing distortion to open the gap. In order to confirm the co-operative nature of the two types of distortions, first-principles total-energy calculations would be necessary in future work.

The present scenario for the charge disproportionation in CaFeO_3 naturally explains why the isoelectronic SrFeO_3 remains free from charge disproportionation: since the ionic radius of Sr^{2+} is large, no tilting distortion is possible for SrFeO_3 and hence the breathing is also blocked. This picture may be analogous to the case of the distorted perovskite BaBiO_3 , in which freezing of a breathing phonon mode is well known [23]. Liechtenstein *et al.* [24] calculated the total energy of BaBiO_3 as a function of tilting and breathing distortions and found that the instability and the gap opening occurs only when the two kinds of distortions are combined; in the presence of the tilting distortion, the nesting instability of the Fermi surface emerges, leading to the alternating breathing distortion of Bi-O octahedra. If the same nesting instability is confirmed for CaFeO_3 by first-principles band-structure calculations, then the quite different mechanism of the charge disproportionation would be established between $\text{La}_{0.33}\text{Sr}_{0.67}\text{FeO}_3$, where the ordering of holes at oxygen sites is purely electronically

driven, and CaFeO_3 , where the lattice distortion and associated electron-phonon coupling is important.

In conclusion, we have shown that the driving force for the charge disproportionation is quite different between the two apparently very similar compounds $\text{La}_{0.33}\text{Sr}_{0.67}\text{FeO}_3$ and CaFeO_3 . The present finding implies that there exists subtle interplay between electron-electron interaction, magnetic interaction, and electron-lattice interaction in realizing charge ordering (or more generally charge inhomogeneity) and charge fluctuations in transition-metal oxides. This means that dominant interaction may change within the same family of compounds, and calls for a critical re-examination of charge ordering/fluctuation phenomena depending on the chemical composition (hole concentration) and crystal distortion even for an apparently similar class of materials.

Discussions with M. Seto and N. Hamada are gratefully acknowledged. This work was supported by a Grant-in-Aid for Scientific Research (A12304018) from the Ministry of Education, Culture, Sports, Science and Technology.

* Present address: Correlated Electron Research Center (CERC), National Institute of Advanced Industrial Science and Technology (AIST), Tsukuba 305-8562, Japan

- [1] J.M. Tranquada, B.J. Sternlieb, J.D. Axe, Y. Nakamura, and S. Uchida, *Nature* **375**, 561 (1995).
- [2] See, e.g., *Colossal Magnetoresistance, Charge Ordering and Related Properties of Manganese Oxides*, ed. C.N.R. Rao and B. Raveau (World Scientific, Singapore, 1998)
- [3] J.A. Alonso, J.L. García-Muñoz, M.T. Fernández-Díaz, M.A.G. Aranda, M.J. Martínez-Lope, and M.T. Casais, *Phys. Rev. Lett.* **82**, 3871 (1999).
- [4] M. Zaghrioui, A. Bulou, P. Lacorre, and P. Laffez, *Phys. Rev. B* **64**, 081102(R) (2001).
- [5] P.M. Woodward, D.E. Cox, E. Moshopoulou, A.W. Sleight, and S. Morimoto, *Phys. Rev. B* **62**, 844 (2000).
- [6] T. Takeda, R. Kanno, Y. Kawamoto, M. Takano, S. Kawasaki, T. Kamiyama, F. Izumi, *Solid State Sci.* **2**, 673 (2000).
- [7] R. Raffaele, H.U. Anderson, D.M. Sparlin, and P.E. Parris, *Phys. Rev. B* **43**, 7991 (1991); J.A.M. Van Roosmalen and E.H.P. Cordfunke, *J. Solid State Chem.* **110**, 109 (1994)
- [8] M. Takano, J. Kawachi, N. Nakanishi, and Y. Takeda, *J. Solid State Chem.* **39**, 75 (1981).
- [9] P.D. Battle, T.C. Gibb, and P. Lightfoot, *J. Solid State Chem.* **84**, 271 (1990).
- [10] J.Q. Li, Y. Matsui, S.-K. Park, and Y. Tokura, *Phys. Rev. Lett.* **79**, 297 (1997).
- [11] A.E. Bocquet, A. Fujimori, T. Mizokawa, T. Saitoh, H. Namatame, S. Suga, N. Kimizuka, Y. Takeda, and M. Takano, *Phys. Rev. B* **45**, 1561 (1992).
- [12] T. Takeda, Y. Yamaguchi, and H. Watanabe, *J. Phys. Soc. Jpn.* **33**, 967 (1972).

- [13] S. Kawasaki, M. Takano, R. Kanno, T. Takeda, and A. Fujimori, J. Phys. Soc. Jpn., **67**, 1529 (1998).
- [14] M. Abbate, G. Zampieri, J. Okamoto, A. Fujimori, S. Kawasaki, and M. Takano, Phys. Rev. B **65**, 165120 (2002).
- [15] M. Takano, S. Nasu, T. Abe, K. Yamamoto, S. Endo, Y. Takeda, and J.B. Goodenough, Phys. Rev. Lett. **67**, 3267 (1991).
- [16] T. Kawakami, S. Nasu, T. Sasaki, K. Kuzushita, S. Morimoto, S. Endo, T. Yamada, S. Kawasaki, and M. Takano, Phys. Rev. Lett. **88**, 037602 (2002).
- [17] G.Kh. Rozenberg, A.P. Milner, M.P. Pasternak, G.R. Hearne, and R.D. Taylor, Phys. Rev. B **58**, 10283 (1998).
- [18] J. Matsuno, T. Mizokawa, A. Fujimori, K. Mamiya, Y. Takeda, S. Kawasaki, and M. Takano, Phys. Rev. B **60**, 4605 (1999).
- [19] T. Mizokawa and A. Fujimori, Phys. Rev. B **54** 5368 (1996).
- [20] L.F. Mattheiss, Phys. Rev. B, **5**, 290 (1972).
- [21] S. Morimoto, T. Yamanaka, and M. Tanaka, Physica B **237-238**, 66 (1997).
- [22] W.A. Harrison, *Electronic Structure and the Properties of Solids* (Dover, New York, 1989)
- [23] S. Uchida, K. Kitazawa, and S. Tanaka, *Phase Transition* (Gordon and Breach Science, New York, 1987), Vol. 8, p.95.
- [24] A.I. Liechtenstein, I.I. Mazin, C.O. Rodriguez, O. Jepsen, O.K. Andersen, and M. Methfessel, Phys. Rev. B **44**, 5388 (1991).